Operational real time geostationary satellite rainfall estimates over the Mediterranean

F. MENEGUZZO[a], B. GOZZINI[b], S. MIGLIORINI[c], , A. ORTOLANI[c], L. BOTTAI[a] & G. ZIPOLI[b]

[a.] F.M.A. - Applied Meteorology Foundation, Via Einstein 35, 50013 Campi Bisenzio (Firenze), Italy – e-mail: meneguzzo@lamma.rete.toscana.it
[b.] National Council of Research, Institute of Agrometeorology and Analysis for Agriculture, Piazzale delle Cascine 18, 50144 Florence, Italy
[c.] LaMMA – Laboratory for Meteorology and Environmental Modeling, Via Einstein 35, 50013 Campi Bisenzio (Firenze), Italy

ABSTRACT

An automated geostationary METEOSAT satellite rainfall estimation technique (the *Neural Rain Estimator*) was developed and operationally applied over Italy and most of central-western Mediterranean to provide half hourly precipitation maps at 0.2 degrees resolution (about 12 x 23 km). The METEOSAT geostationary satellite long-wave infrared (IR) channel observations are the primary data source, since they provide the needed information about cloud top temperatures at a high frequency and fine spatial resolution. The moisture profiles of the environment, in which the precipitation systems develop, are generated by a Numerical Weather Prediction (NWP) model and taken into account due to their effect on the precipitation mechanisms. Neural network algorithms are then applied to connect the selected predictors to ground rainfall, as observed by a rain gauge network in Tuscany, Italy.
The *Neural Rain Estimator* provides a relevant added value information with respect to the original METEOSAT imagery and may represent a routinely available tool for NWP model validation and numerical initialization.

1 INTRODUCTION

Several relevant reasons can be identified to develop, operate and maintain a service of high frequency satellite rainfall estimates over relatively large areas, especially if they involve marine and/or partly unmonitored covered regions. The most obvious reason is the production of quantitative information about current rainfall systems, directly utilizable by weather forecasters and operational hydrologists, providing value added information with respect to the (calibrated) Meteosat imagery (e.g. Levizzani *et al.*, 1996; Vicente *et al.,* 1998). Another relevant use of the satellite rainfall maps is the crop yield forecasting in marginal areas, e.g. the Sahel region. Furthermore, the accurate evaluation of the daily forest fire risk needs accurate knowledge of the previous dry days series (number of consecutive days with rainfall below a predefined threshold), often very difficult to obtain in real time over largely unmonitored areas (e.g. Maracchi *et al.*, 1998). Rainfall climatology is often characterized by large uncertainties over unmonitored and marine areas; the evaluation of the water cycle trends over such regions, particularly relevant in the frame of the global climate change, and the validation/calibration of the seasonal forecasts are thus often unreliable (e.g. Grifoni *et al.*, 1998). High frequency satellite rainfall estimates can cover these deficiencies.

Other important uses of the high frequency rainfall maps over large areas are the validation and physical initialization of numerical weather prediction (NWP) models. Manobianco *et al.* (1993) have dynamically assimilated satellite-derived precipitation into a regional scale model by scaling the internally generated model profiles of latent heating for the simulation of tropical cyclones. Simulations showed that satellite precipitation does not induce noise during or after the assimilation period, forces the model to reproduce the magnitude and distribution of satellite rainfall patterns, and improves the simulated mean sea level pressure (MSLP) minima, frontal positions and the low-level vertical-motion patterns. The model retains information from the assimilation up to 8.5 hours after the end of the assimilation itself. A multivariate optimal interpolation analysis was applied by Turk *et al.* (1999) to the physical initialization of the Naval Operational Global Atmospheric Prediction System (NOGAPS) for the nowcasting of tropical precipitation. Added accuracy, better location and intensity of convective precipitation were found to lead to an improvement in the NOGAPS assimilation rain rates as verified against satellite observations. A significant improvement in the forecasts of precipitation patterns, MSLP fields, and geopotential height fields was found also in this extra-tropical case.

Results generally indicate that a positive impact of non-conventional satellite input data, especially precipitation, into numerical weather prediction models exists, with a significant impact on the quantitative precipitation forecasts.

Since the 1960s, several techniques were developed to estimate surface rainfall based on visible (VIS) and infrared (IR) imagery collected by geostationary satellites (*Lovejoy et al.*, 1979; *Barrett et al.*, 1986; *Adler et al.*, 1988; *Goodman et al.*, 1994). The relevance of IR imagery to the rainfall estimation is demonstrated by the evidence that intense thunderstorms are characterized by very cold cloud top temperatures and rapid changes in time and in space on the structure of the cloud top surface (*Vicente et al.,* 1996).
Techniques aimed at the estimation of rainfall over quite long time periods (e.g. monthly) and over large areas often use crude threshold methods, while random errors are reduced by the large integration scale itself. If conservation of good performances at short time aggregations is a strict requirement, finer analyses are needed. *Hsu et al.* (1997), for example, stress the seasonal and site specific dependence of the relationships between rainfall and cloud top brightness temperature.Several techniques have been developed with similar aims. Some of them are designed on a pixel by pixel basis, but generally employ only satellite information, are site and season specific, sometimes use adaptive calibration with radar and/or rain gauge observations. Inter-calibration of satellite estimates is in this respect, also a relevant topic. *Levizzani et al.* (1996) highlight the role of the Special Sensor Microwave / Imager (SSM/I) passive microwave sensor which performs a far more direct observation of cloud and rain structure and, if suitable algorithms are employed, rain maps derived from SSM/I may be used for the validation of the METEOSAT estimates. Unfortunately such technique cannot be used for flash flood warnings due to the low frequency of observation. In a recent work (*Hsu et al.*, 1997), artificial neural networks were employed for off-line and adaptive calibration of satellite estimates (i.e., calibration of the rainfall estimates "on the fly" with the available updated rain gauge and radar observations). In the frame of this technique, the specific environmental conditions were not considered and good performances were obtained only activating the adaptive option, especially in the mid-latitudes. If no adaptive algorithms are used (either due to difficult data access, sparse or insufficient rain gauge or radar data), the assimilation of environmental conditions is needed.
This work illustrates the architecture, data, performances and some derived applications of the automatic satellite rainfall estimation technique over the central-western Mediterranean.

2 METHODOLOGY

The goal of the *Neural Rain Estimator* is to diagnose the half hourly ground rainfall. The thermal infrared (IR) data provided by the geostationary satellite (Meteosat-6 and -7 for the Mediterranean area) observations each half hour are georeferentiated by means of an accurate orbital method and displayed on a 0.2° x 0.2° spatial resolution grid. Such data are then assimilated and processed on a

pixel by pixel basis to identify some relevant features of the cloud top evolution and structure: brightness temperature, growth rate (in K per half hour), overshooting tops and sinking areas (after a finite difference analysis of the cloud top temperature through the local Hessian matrix) and horizontal gradient. Furthermore, a finer scale analysis has been provided, georeferentiating the whole scene at 0.04° x 0.04°, approximately the original METEOSAT spatial resolution. In this way, for every aggregated pixel – composed by a 5 x 5 subpixel grid – standard deviation of brightness temperature is calculated and added to the selected cloud features. These features have been recognized as especially important to perform a screening of non-raining pixels (*Woodley et al.*, 1972; *Scofield,* 1977; *Adler et al.*, 1988).

In the development of the *Neural Rain Estimator*, the METEOSAT infrared imagery is processed to identify several key features of the cloud systems. An important topic is the screening of cloudy and clear pixels: soil and sea surface temperatures are taken from an NWP model short term forecasts and the cloud threshold is taken 10 K below the surface temperature, with an absolute threshold of 273 K to consider only clouds with ice phase. Such threshold was selected after an accurate analysis of the solution of the radiative transfer equation for thermal infrared, represented by a relationship between brightness temperature at the top of the atmosphere and surface temperature (fig. 1).

A neural network was first calibrated to screen the pixels and identify the rainy ones. A second network was calibrated to provide the rainfall depth over the desired time period (30 minutes), only over estimated rainy pixels. The input data for both networks were derived from the analysis of the satellite imagery and from meteorological model data.

Since both neural networks get the input data from the three involved satellite scenes, it is necessary to screen all the situations that the networks may face. Most of the rainfall events (i.e. half an hour with rainfall over a specific pixel) occurred with cloudy conditions in all the three satellite scenes, and the cases with clear sky at least in the last two satellite scenes had zero rainfall in the last 30 minutes. The other combinations involved a small number of cases and simple linear or exponential regressions were used to derive the probability of rainfall occurrence (screening of rainy pixels) and the quantitative rainfall estimation on the basis of the useful satellite and meteorological model data.

The neural network belongs to the multi-layer perceptron (MLP) global neural network model (*Lawrence et al.*, 1996) and uses the backpropagation tool. The backpropagation is an extremely effective learning tool that can be applied to a wide variety of problems; its related paradigms require supervised training. This means they need a set of training data where known solutions are supplied.

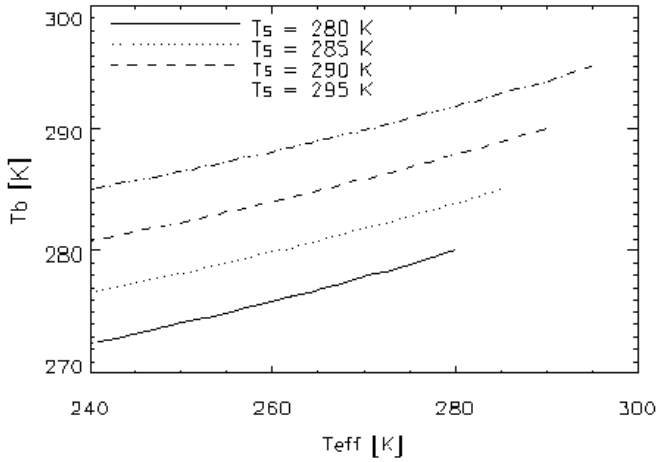

Figure 1: Brightness temperature T_b at the top of atmosphere as a function of T_{eff}, atmospheric effective temperature, relative – for the atmospheric window channel - to a pressure level near to the surface. Different plots are for typical surface temperature values T_s. To be noted that the difference between T_b and T_s is always lower than 10 K.

3 DATA ANALYSIS

Fig. 2 shows the area covered by both METEOSAT IR imagery and meteorological model data and the calibration area, which roughly corresponds to Tuscany, Italy. METEOSAT infrared, meteorological model and ground rainfall data were collected during more than twenty storm events occurred in 1997 and 1998.Georeferentiation assured an accurate correspondence between satellite and ground data (errors less than the original METEOSAT infrared pixel size).

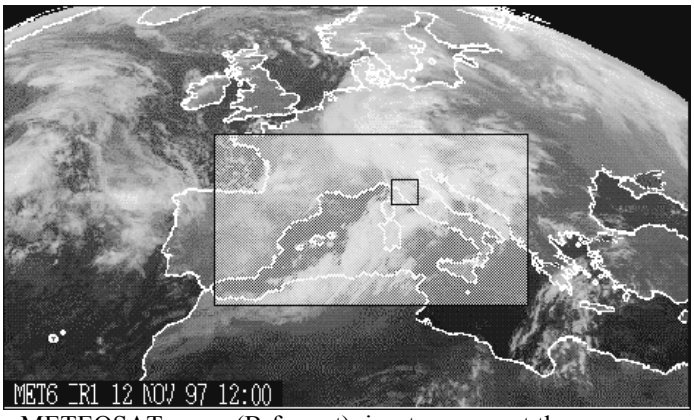

Figure 2: METEOSAT scene (B-format); insets represent the area covered by the meteorological model data (outer rectangle) and the calibration area (inner rectangle).

Time series of quantities from the METEOSAT IR scenes on a pixel by pixel basis were produced, namely brightness temperatures and cloud top structures (gradient, convexity, concavity or saddle) of each series of three temporally consecutive scenes. Time series of simultaneous meteorological model derived data were also worked out. In particular was calculated the product of the precipitable water (PW) and relative humidity (RH), both computed in the layer surface to 500 hPA, divided by 1000, i.e. the PWRH factor. Both PW and RH are computed from the short time forecast atmospheric fields from a limited area model (DALAM model) nested into the global circulation model of the European Center for Medium range Weather Forecasts (ECMWF) and running over the southern Europe and Mediterranean basin (*Buzzi,* 1994; *Perini et al.,* 1995). The atmospheric fields are available at the time resolution of 3 hours and the quantities PW and RH are interpolated in time to get the mean value over the time interval between the first and the last of the three METEOSAT scenes (one hour).

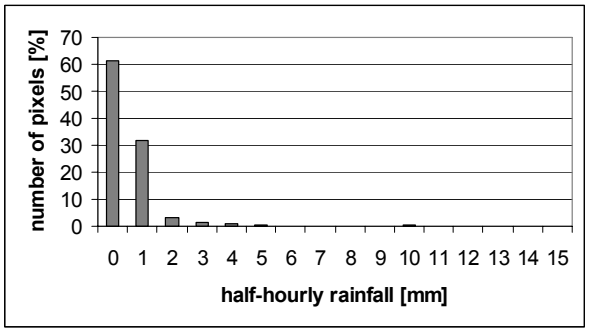

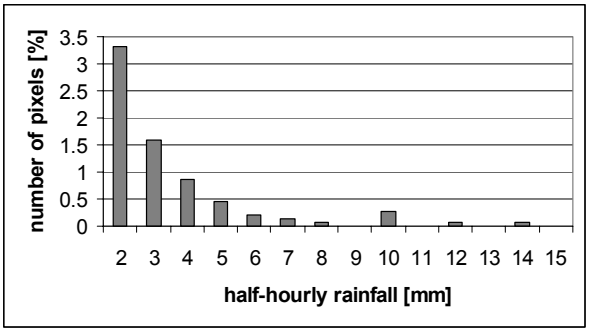

Figure 3: (a) Relative frequency of the rainfall values in 30 minutes over the pixels 0.2° longitude by 0.2° latitude over the whole data set (1510 data); (b) same as (a), extended scale.

Time series of thirty minutes cumulated rainfalls at the rain gauges were also collected and averaged over the selected pixels by means of simple arithmetic means from the data at the rain gauges. Fig. 3a e fig. 3b show in two different scales the relative frequency of the rainfall values over the whole data set,

which consists of 1510 records of satellite infrared, meteorological model and rain gauge interpolated data; the rainfall data are apparently concentrated in the lower part of the range, which represents a limit to the calibration of the neural network over heavy rainfall events.

(a)

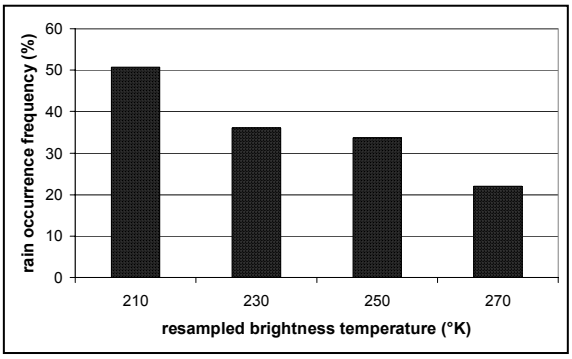

(b)

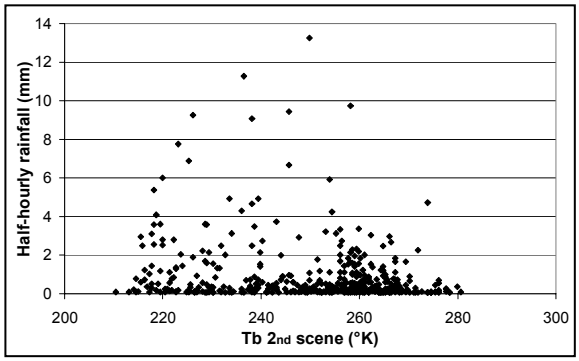

(c)

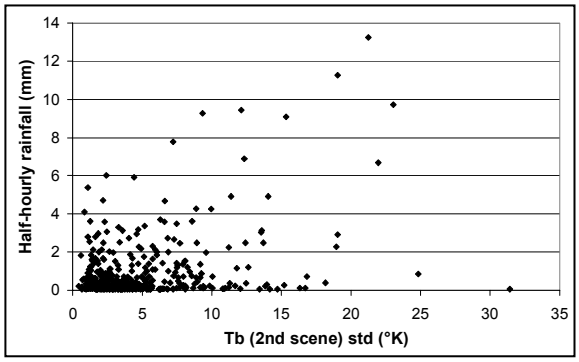

Figure 4: Relationship between rainfall in 30' minutes (greater than 0.04 mm) and (a) cloud top temperature (b) cloud top brightness temperature standard deviation at the beginning of the thirty minutes rain period (2nd scene), (c) brightness temperature at the end of the rainy period.

Preliminary data analysis was aimed to the identification of clear relationships between cloud top features and ground rainfall. The relative frequency of rain occurrence was compared on a pixel by pixel basis to resampled cloud top temperature in the second METEOSAT IR scene, at the beginning of the thirty minutes rain period (Fig. 4.a). It was also compared to the cloud top brightness temperature standard deviation in the second (Fig. 4.b) and brightness temperature in the third scene, just at the end of the rainy period (Fig. 4.c).
It is revealed a greater frequency of rainy events in the lowest cloud top temperature range (Fig.4.a) and a greater intensity in the same range (Fig. 4.b) and for higher standard deviation values (Fig. 4.c) or in presence of convective activity at smaller scale, in agreement with the results previously found by *Vicente et al.* (1996).

4 RESULTS AND DISCUSSION

The two neural networks employed in the development of the new methodology were designed separately both for the best performance on the independent test data sets and the stability.
The best performance and stability of the network trained over the binary data set (rain / no rain) were obtained with the configuration set at one hidden layer with fifteen input nodes and twenty hidden nodes. The best performance and stability of the network trained over the rainfall amounts computed for the pixels where actually rainfall occurred were obtained with the configuration set at one hidden layers with ten input nodes and fourteen hidden nodes. This facts were established after several comprehensive trials using the same partition of the whole data set between the validation and the test sets. Furthermore, selection of the predictors for the neural network was established by means of the Wilcoxon two sample test (Wilks, 1995).
The performances of the two neural networks were evaluated by means of the same statistical indices as the Auto-Estimator, but the target quantity is the rainfall (occurrence and amount) in 30 minutes. A lower limit for the half-hourly rainfall was set to 0.04 mm, equal to the estimated a priori rain-gauge error – 0.2 mm – divided by five, the minimum number of raingauges in a resampled pixel. Since the "screening" network was trained over binary target data (0 for no rainfall, 1 for rainfall), the outputs from the network were interpreted as probability of occurrence of the rainfall. A major problem was thus the choice of the output threshold which allowed the best couple of values of the *probability of detection* (POD) and *false alarm ratio* (FAR). A possible solution is to study the *critical success index* (CSI) and to get as threshold the probability of maximum CSI (fig. 5). Such criterion implies a probability threshold of 0.33 - an output from the network smaller than 0.33 means no rainfall, otherwise rainfall - corresponding to a POD of 64.0 % and a FAR of 52.9 %. It should be noted that such choice, even if statistically well based, is

somewhat arbitrary and can change in case of greater importance of false alarm with respect to the probability of detection or viceversa.
To select the predictors of the network for the quantitative rain estimation, a forward stepwise multi-regression was provided to the whole data-set. Only variables that were able to improve the correlation coefficient have been retained. At the end of the training process, a squared correlation coefficient R^2 = 0.44 was obtained over the test set (fig. 6).
Some more words may be spent about the underlying physics revealed after the identification of the best configurations of the two neural networks.

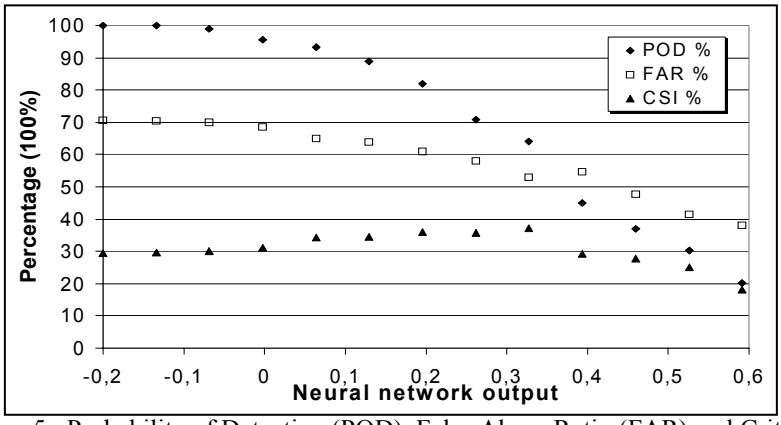

Figure 5: Probability of Detection (POD), False Alarm Ratio (FAR) and Critical Success Index (CSI) relative to rain detection (greater than 0.04 mm) as a function of neural network estimator normalized output.

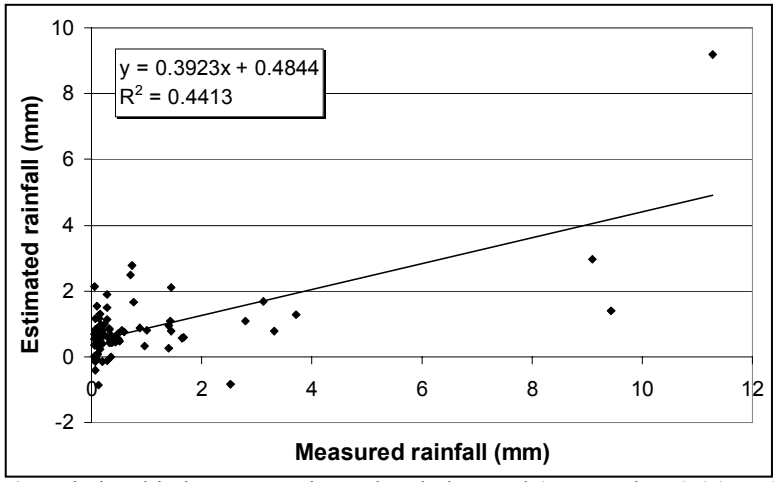

Figure 6: Relationship between estimated and observed (greater then 0.04 mm) half-hourly rain as resulted from the second neural network, for rainy data with binary threshold equal to 0.03. Resulting squared correlation R^2 = 0.44.

The classes of input data which play the most relevant role in the screening of the rainy pixels are the cloud top temperature rates during the hourly time period between the first and the last satellite scene at the half hour time step.
The occurrence of very cold cloud top temperatures at the beginning of the half hour is in most cases sufficient to diagnose rainfall in the following half hour.
Four classes of input data play the most relevant role in the diagnose of the rainfall amount. In decreasing order of relevance, they are the standard deviation of the cloud top temperature and the cloud top temperature in the third satellite scene (at the end of the rainfall estimation period), the standard deviation of the cloud top temperature in the second satellite scene (at the beginning of the rainfall estimation period) and the cloud top temperature in the first satellite scene.
From these results seems clear that if a cold cloud top temperature at the beginning of the last half hour is able to produce the raining event, the amount of rainfall depends on the concurrence of cold cloud top temperature in the whole hour and on the degree of subpixel temperature unhomogeneity, correlated to convective motions at smaller scale.

5 SYSTEM ARCHITECTURE

The aim of the entire operational system is to process the input satellite and meteorological model data for producing a set of files, containing real-time updated information on the rainfall quantities, in an easy-to-use interface. Specifically the system outputs are a set of GIF images for the rain quantity fallen in the last 0.5, 1, 3, 6, 12 and 24 hours, and an animation (in GIF format) of the last 6 hours with 30 minutes steps. All these output images are managed by an HTML page, containing also explicative information, and they are available on WEB (http://www.lamma.rete.toscana.it/previ/ita/rainprev.html).
The system has overall to manage:

- the input of a heterogeneous data set,
- the checking phase on data availability and update state (when foreseen),
- the real-time data processing flow (by means of a number of procedures and interface files),
- the checking phase on each processing step success,
- the output files,
- the transferring operations to their final locations,
- the checking phase on data refresh for the output interface,
- its own refreshing and restarting in case of sudden interruption of the normal processing flow.

The system structure is given in fig. 8: METEOSAT and meteorological data model arrive at the UNIX central unit (SERVER) by means of independent programs, as soon as they are available. Here a timed procedure (the main one)

performs all the steps that, from the input data, produce the rainfall GIF images, and transfer such images on the WEB machine. On the WEB there is a second independent timed procedure, which checks the update state of the rainfall quantity images: when the images are older than a given time (due to any kind of problem in the system flow), they are substituted with an emergency image informing any WEB user of the update interruption; at the same time an e-mail message is sent to the system responsible.
The main procedure running on the SERVER, is a C program that each half-hour reads the machine time, then writes and runs a number of UNIX scripts for C shell. The scripts contain all the command steps for the data processing, with the appropriate names for the input and output files which depend on the time they refer. The advantage to have different scripts for each half-hour (corresponding to the update time of the METEOSAT and meteorological model data) is that such scripts can be run independently also a few hours after they have been generated. In addition the scripts have some checking steps which make them not working if the input data are not all available or the scripts have already run with success. With this architecture the system each 5 min. tries running the scripts produced in the last 12 hours without making the machine CPU working if not necessary, consequently it updates the output data no later than 5 min. after the input one are available, and it recovers any past computations (within 12 hours) accidentally interrupted, when all the necessary conditions are restored.

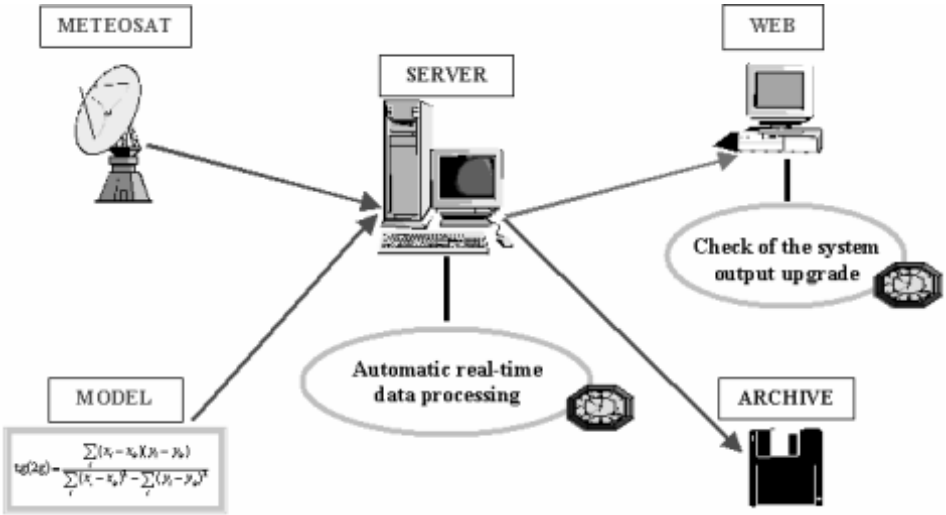

Figure 7: Operational system architecture (see text for details).

6 CONCLUSIONS

New perspectives for several environmental fields are opened by the automatically estimate of rainfall from routinely available geosynchronous satellite infrared data and meteorological model data. In operational weather forecasting, natural applications are the early warnings for flood and flash flood events and local scale weather nowcasting.
In applied meteorology, the early estimation of accumulated rainfall over fire hazardous areas and large marginal areas from routinely available information may be of critical relevance for operations and planning. Particularly important is the design of a suitable technique for the screening of rainy pixels: large errors in this phase may lead to unrealistic over- or under-estimations of the area coverage of a precipitation system. The neural network approach has revealed a considerable skill in this respect.
The verification of the quantitative diagnosis of the rainfall may be affected by some random errors due to the use of rain gauge data, which leads to interpolation errors when the rainfall is evaluated over relatively large pixels (in this case 0.2 longitude by 0.2° latitude). Results are anyway encouraging, even if the performances are hard to evaluate due to the lack of data in the higher range of rainfall amounts. In particular, binary results are sensibly better than correspondent half-hourly results: this is very reasonable due to the fact that in a rainy day there are forty-eight possibility to detect rain, increasing in this way the overall probability of detection of the events. Better false alarm ratio for daily rain is instead explained by the fact that a non-rainy day is more effectively detected than a non-rainy half hour within a rainy event. Performances of the quantitative rain estimation depend only on the ability of the neural network to map the measured rainfall range. Results obtained in the different time intervals present the almost same accuracy: this fact is correlated to the low degree of dispersion of the obtained half-hourly estimates with respect to the measured ones.
Tuscany, Italy, like many other areas in the Mediterranean countries, is prone to flash flood events due to the peculiar hydrography and orography. While extensive rain gauge networks are routinely operated during heavy rainfall events, few calibrated weather radar systems are installed and their data accessed in real time. Satellite rainfall estimates may thus represent a substantial improvement in this respect, as regards both to quantity and spatial structure of precipitation systems over medium-large size basins (300-400 Km^2 and up).
Present hydrological models require distributed input data in terms of the main characteristics of the basin and fine spatial resolution in terms of rainfall data. The methodologies analyzed in this work may be of great importance for real

time flash flood warnings, especially when they will be coupled with calibrated rainfall-runoff models.
The next task is to calibrate the neural networks and verify the methodology over larger data sets; the need for rainfall amounts covering a wider range, especially at higher values, is particularly urgent.

ACKNOWLEDGMENTS

Dr. Vento and Dr. Perini (MiPA-UCEA, Italian Ministry for Agriculture) are gratefully acknowledged for the provision of limited area model data.
Dr. Col. Sorani and Dr. Col De Leonibus (ITAV, Italian Air Force) are gratefully acknowledged for the provision of part of satellite infrared imagery.

REFERENCES

Adler, F.R., and AJ. Negri, A Satellite Infrared Technique to Estimate Tropical Convective and Stratiform Rainfall, *J. Appl. Meteor., 27,* 30-51, 1988.

Barret, E.C., G. D'Souza, and C.H. Power, Bristol Techniques for the Use of satellite Data in Raincloud and Rainfall Monitoring ,. *J. Br. Interplantet. Soc., 39,* 517-526, 1986.

Buzzi, A., Validation of a Limited Area Model in Cases of Mediterranean Cyclogenesis: Surface Fileds and Precipitation Scores, *Meteorol. Atmos. Phys., 53,* 137-153, 1994.

Goodman, B., D.W. Martin, W.P. Menzel, and E.C. Cutrim, A Non-linear algorythm for estimating 3-hourly rain rates over Amazonia from GOES/VISSR observations, *Remote Sensing Reviews, 10,* 169-177 1994.

Grifoni, D., F. Meneguzzo, B. Gozzini, A. Crisci and G. Zipoli, Relationship between large scale atmospheric processes, sea surface temperature patterns and regional basin scale monthly rainfall, *7th ICCTA – International Congress for Computer Technology in Agriculture*, Florence, 15-18 November 1998.

Hsu, K.-L., X. Gao, S. Sorooshian, and H.V. Gupta, Precipitation Estimates from remotely Sensed Information Using Artificial Neural Networks, *J. Appl. Meteor, 36,* 1176-1190, 1997.

Lawrence, S., A.C. Tsoi, and A.D. Back, Function Approximation with Neural Networks and Local Methods: Bias, Variance and Smoothness, Appears in Australian Conference on Neural Networks, ACNN 96, Edited by Peter Bartlett, Anthony Burkitt and Robert Williamson, Australian National University, pp. 16-21, 1996.

Levizzani, V., F. Porcù,, F.S. Marzano, A. Mugnai, E.A. Smith, and F. Prodi, Investigating a SSM/I Microwave Algorithm to Calibrate Meteosat Infrared Instantaneous Rainrate Estimates. *Meteorol. Appl., 3,* 5-17, 1996.

Lovejoy, S., and G. L. Austin, The Delineation of Rain Areas Satellite Infrared Technique to Estimate Tropical Convective and Stratiform Rainfall. *J. Appl. Meteor., 27,* 30-51, 1979.

Perini, L., A. Brunetti, and D. Vento, Il Modello ad Area Limitata del Ministero delle Risorse Agricole, Alimentari e Forestali. *AER, 11,* 21-25, 1995.

Maracchi, G., and R. Costantini, 1998. A Meteorological Model for Forest Fire Forecast in Tuscany. Proceedings of III International Conference on Forest Fire Research "Forest Fire Resarch", Coimbra 16/20 November 1988, Portugal. Edited by: D. X. Viegas, ADAI Univ. Coimbra, Portugal, 1085-1098.

Manobianco, J., S.E. Koch, V.M. Karyampudi and A.J. Negri, 1993. The Impact of Assimilating SSM/I and GOES/IR Derived Precipitation Rates on Numerical Simulations of the ERICA IOP 4 Cyclone. *Mon. Wea. Rev.*

Scofield, R.A., and V.J. Oliver, A scheme for estimating convective rainfall from satellite imagery. *NOAA Tech. Memo. NESS86*, U.S. Dept. Commerce, Washington, DC, USA, 47 pp, 1977.

Turk,F.J., G.D.Rohaly, J.Hawkins, E.A.Smith, F.S.Marzano, A.Mugnai and V.Levizzani, 1999. Meteorological applications of precipitation estimation from combined SSM/I, TRMM and infrared geostationary satellite data. *6th Specialist Meeting on Microwave Radiometry and Remote Sensing of the Environment*, Florence, Italy, 16-18 March, in press.

Vicente, G.A., and R.A. Scofield, Experimental GOES-8/9 Derived Rainfall Estimates for Flash Flood And Hydrological Applications. Proceedings of the 1996 Meteorological Satellite Data Users' Conference. Vienna Austria, 16^{th}-20^{th} September 1996. EUM P 19, pp. 89-96, 1996.

Vicente, G.A., and R.A. Scofield, Satellite Rainfall Estimates in Real Time Through the Internet for Applications to Flash Flood Watches and Warnings and Heavy Precipitation Forecasting. Proceedings of the Earth Observation & Environmental Information (EOEI'97) conference. Alexandria, Egypt, October 13-16, 1997.

Vicente, G.A., R.A. Scofield, and W.P. Menzel, The Operational GOES Infrared Rainfall Estimation Technique. Accepted for Publication in the: Bulletin of the American Meteorological Society, September edition, 1998.

Wilks S.D. Statistical Methods in the Atmospheric Sciences, 467 pp., Academic Press, San Diego, 1995.

Woodley, W.L., B. Sancho, and A.H. Miller, Rainfall estimation from satellite cloud photographs. *NOAA Tech. Memo. ERL OD-11*, 43 pp., 1972.